



## Percolation Behavior of Conductor-Insulator Composites with Varying Aspect Ratio of Conductive Fiber

JAE YEON YI & GYEONG MAN CHOI

*Department of Materials Science and Engineering, Pohang University of Science and Technology, Pohang, 790-784, Korea*

Submitted January 22, 1999; Revised May 27, 1999; Accepted June 4, 1999

**Abstract.** The electrical properties of composite electroceramics are determined by the concentration, shape and distribution of filler phase in matrix. The carbon fiber-filled polymer was chosen as a model system and the electrical conductivity was measured as a function of carbon fiber content and the aspect ratio (AR) of the fibers to understand the percolation behavior of the composites. The composites of carbon fiber (1 ~ 9 vol.%) and thermoplastic polymer were fabricated in a mold press with the aspect ratio of carbon fiber varying between 4 and 10. The percolation threshold volume concentrations ( $V_c$ ) of transition from the insulator to the conductor decreased as the fiber aspect ratio increased. With the fibers segregated at the polymer-polymer interfaces in the present study,  $V_c$  values were much smaller than those with the fibers randomly distributed in the matrix shown in other studies. The inverse relation between  $V_c$  and AR was found as expected. From the comparison with other experimental and simulated data, we concluded that the slope in  $1/V_c$  versus AR plot is a strong function of fiber segregation.

**Keywords:** percolation, fiber, composite, aspect ratio, conductivity

### Introduction

Composite materials are generally known to have many structural applications, but their use in electronics has been relatively limited. However, composite electroceramics have recently been used in increasing number of applications such as thermistors, piezoelectric ceramics, and sensors etc.. The principles and applications of a wide range of composite electroceramics have been reviewed elsewhere [1,2]. In many applications of composite, the electrical resistivity is a main variable and thus the electrical conductivity of composite has also been reviewed recently [3]. It was shown that effective media and percolation theories can be used to describe the electrical resistivity of composite [3]. The same theories can be used to explain other physical properties, such as thermal conductivities, diffusion constants and permeabilities of multiphase materials [3]. Although the direct determination of other physical properties, that are much harder to measure,

from the determination of electrical conductivity is not straight forward, a similar trend may be observed in their concentration dependence. For example, the percolation threshold concentration of the thermal conductivity may be estimated from the electrical measurement of composites containing highly electrically and thermally conductive fillers [4,5]. The same percolation concentration has been observed between electrical conductivity and dielectric permeability [6,7].

Composite electroceramics may be composed of ceramic filler and polymer matrix as well as ceramic filler and ceramic matrix. The polymer-ceramic composite has many similar applications as shown for ceramic-ceramic composite, such as thermistors and piezoelectrics [1–3]. The ceramic fillers in a polymer matrix may be spherical particles, thin plates, or fibers. The composites with spherical particles are most studied due to their ease of fabrication and availability. The use of asymmetric fillers with aspect ratio greater than 1 reduces the volume fraction of

fillers needed for conduction, and often improves the mechanical properties of the resulting composites. The resistivity of polymer-fiber composites is also expected to be a sensitive function of the distribution of conductive fiber fillers as shown in the composites containing spherical fillers [8,9].

Although many polymer materials are insulators, electrically conductive polymers have also many applications in a variety of areas such as shielding of electromagnetic fields in electronic instruments [10–13]. The principal techniques for making conductive polymers include the synthesis of electronically conducting polymers, the incorporation of metallic particles in a polymer by thermal decomposition of specific metal-organic compounds, the implantation of metal, and compounding of a polymer with conductive fillers. In this study, the composites of spherical polymer particles and conductive fibers were fabricated with controlled microstructure and their conductivity and percolation behavior was studied. Polymers with conductive fibers also serve to test the percolation behavior of insulator-conductor composites. The electrical conductivity of composites, consisting of insulating polymer and conductive fillers, does not increase monotonously with increasing filler content, but there is a critical volume concentration ( $V_c$ ), so called percolation threshold volume concentration, where the resistivity of the composite drops abruptly from the insulating ( $>10^{10}\Omega\text{ cm}$ ) to the semiconducting or conducting ( $<10^5\Omega\text{ cm}$ ) state due to the formation of a continuous filler network as the filler content increases [12,14]. The filler may be spherical particles or non-spherical objects such as fibers or plates with various degree of non-symmetrical shape. The excluded volume [15] of the percolating objective has been emphasized for making predictions [16,17] for non-spherical particles. The excluded volume of an object is defined as the volume around an object into which the center of another similar object is not allowed to enter if overlapping of the two object is to be avoided [15]. If the excluded volume of two conducting fibers overlap, there is a certain probability that they will form a conducting link. Thus only a small volume fraction of fibers with their inherently high excluded volume is needed to make the polymer-carbon fiber composite conductive. The theoretical calculation showed that the aspect ratio ( $AR = \text{length}(l)/\text{diameter}(d)$ ) dependence of the critical volume percentage for very thin sticks or fibers is  $V_c \propto (AR)^{-1}$  [15,16]. A reported

experimental result of the aspect ratio dependence on the critical volume percent of randomly oriented thin sticks showed a deviation from the above prediction [4]. In addition, different  $V_c$  values were reported for the samples with different polymer matrix but same filler fibers [4]. Thus, the dependence of  $V_c$  on the aspect ratio is not entirely clear and a part of the discrepancy may be due to the difference in the details of experimental condition.

In this study, we investigated the variation of the critical volume percentage by measuring the electrical conductivity of the composites with varying fiber aspect ratio and by fitting the conductivity curves with general effective medium (GEM) equation [3]. We also modified the microstructure of composite to obtain the conductive composite with the minimum amount of conductive filler fibers. The variation of critical volume concentration or percolation threshold concentration was explained in relation with the microstructure. The variables of GEM equation were also discussed.

## Experimental

The matrix material was spherical polymer (Acrylic thermoplastic resin No. 3, Struers Co., Denmark) particle (average particle size:  $103.4 \pm 34.8\ \mu\text{m}$ ) and the filler was carbon-fiber (Toray Co., Japan) of  $8\ \mu\text{m}$  diameter. The aspect ratio of the carbon fibers was controlled before adding the fibers into the polymer. Carbon fibers were crushed by rolling magnetic bars in a jar, filled with fibers and classified by varying the crushing time and followed by sieving. Thus four aspect ratios varying between 4 and 10 were obtained. After measuring the length of 1000~1500 crushed fibers in each group using optical microscope(OM), both the aspect ratio and the standard deviation for each classified fiber group were determined.

The density of polymer particles was measured by the floating method. After dispersing the particles in salt water and successively controlling the salt to water ratio to float the polymer particles uniformly for 2 h, the density of salt water was measured. The polymer particles and fibers with varying fiber content between 1 and 9 vol.% were mixed in a rolling plastic bottle for 12 h. The disk-shaped composites of 30 mm diameter were fabricated with a mold press at  $180^\circ\text{C}$ , 140 MPa for 30 min. 5–8 samples containing 1–9 vol.% of carbon fibers were fabricated for each aspect

ratio. The polished surfaces of composites were observed using OM. About  $5 \times 5 \times 5 \text{ mm}^3$  cube was obtained by cutting with diamond saw and two opposite sides of the cube were polished with SiC paper (#1200). Ag electrode (Dupont, No. 4922, USA) was pasted on both sides and the specimens were heat treated at  $100^\circ\text{C}$  for 1 h.

The electrical resistance values of the specimens were measured at room temperature by 2-probe dc method using high voltage source/measure unit (Keithley, Model 237, USA). The electrical resistance (R) value of the specimen was calculated using current-voltage curves and the applied voltage range varied  $-1 \sim +1 \text{ V}$  to  $-1000 \sim +1000 \text{ V}$ . The electrical conductivity ( $\sigma$ ) was calculated by

$$\sigma = \frac{t}{A \cdot R} \quad (1)$$

where  $A$  and  $t$  represent the electrode area and the thickness of the specimen, respectively. The electrical conductivity of a single carbon-fiber was measured by a probe station (Cascade Microtech., REL-3200, USA) using 4-probe dc method.

The electrical conductivity values were plotted versus fiber content and the curves were fitted with the general effective medium (GEM) equation [3]:

$$\frac{(1 - V_c)(\sigma_p^{1/t} - \sigma_m^{1/t})}{\sigma_p^{1/t} + \left(\frac{1-V_c}{V_c}\right)\sigma_m^{1/t}} + \frac{V_c(\sigma_f^{1/t} - \sigma_m^{1/t})}{\sigma_f^{1/t} + \left(\frac{1-V_c}{V_c}\right)\sigma_m^{1/t}} = 0 \quad (2)$$

where  $V_c$  and  $t$  represent the critical volume concentration (or percolation threshold concentration) of fibers and the morphological variable of GEM equation, respectively, and  $\sigma_f$ ,  $\sigma_p$  and  $\sigma_m$  represent the electrical conductivity of carbon-fiber, polymer and composite, respectively.

## Results and Discussion

The density of the polymer particles was measured to be  $1.19 \text{ g/cm}^3$ , and that of the carbon fibers was found to be  $1.86 \text{ g/cm}^3$  [18], respectively. The measured densities of the specimens were compared with the theoretical densities ( $d_{\text{theo}}$ ) of composites obtained from the rule of mixture,

$$d_{\text{theo}} = d_p \cdot V_p + d_f \cdot V_f \quad (3)$$

where  $d_p$ ,  $d_f$  and  $V_p$ ,  $V_f$  represent the densities and the volume fractions of polymer particles and fibers,

respectively. The relative densities were about 98% of the theoretical densities invariant of carbon-fiber content varying from 1 to 9 vol.%. Carbon-fiber addition prevented very little of polymer compaction.

Figure 1 shows the morphologies of classified carbon fibers for each aspect ratio. Fibers were dispersed in alcohol and dried on alumina plate for observation. The length of fibers was measured from the optical micrographs of the classified fibers. The size distribution curves of fibers are shown in Fig. 2. The most frequent sizes and average sizes are shown and vertical lines are average size and  $\pm$  one standard deviation. As shown in Fig. 2, the measured average aspect ratios ( $\pm$  standard deviations) are (a)  $4.0 (\pm 2.1)$ , (b)  $6.9 (\pm 3.2)$ , (c)  $8.9 (\pm 4.9)$  and (d)  $10.3 (\pm 6.1)$ , respectively. A few very long fibers are found in each group and the distribution curves show asymmetric shapes.

Figure 3 shows optical micrographs of polished surface of the composites for the fiber aspect ratio of 6.9 and vol.% varying (a) 3.0, (b) 5.4, and (c) 7.8. In Fig. 3(c), the dotted circles were drawn to help the identification of polymer particles. As shown, the white-colored carbon fibers do not penetrate the polymer particles but are located at the boundaries between them. No preferential segregation of the fibers in a particular direction was observed from the fractured surfaces of the samples. Although the degree of interconnection increased with the fiber volume percent, no electrode-to-electrode connection of fibers is evident in two-dimensional micrographs. However, the increasing connectivity was found in a sequence of Fig. 3(a), 3(b), and 3(c).

In Fig. 4, the electrical conductivities of composites with aspect ratio of 4.0, 6.9, 8.9, 10.3 are shown as a function of fiber content. Symbols represent the measured conductivity values and lines represent GEM fitting curves. The electrical conductivity of a polymer [19] is generally  $10^{-17} \sim 10^{-15} \Omega^{-1} \text{ cm}^{-1}$  and that of the carbon fiber [20] may vary depending upon manufacturing condition. The measured conductivity of the carbon-fiber by the probe station was  $93 \Omega^{-1} \text{ cm}^{-1}$ . The morphological variable ( $t$ ) and critical volume percent ( $V_c$ ) or percolation threshold concentration are summarized for each aspect ratio in Table 1. The experimental data was nicely fitted with GEM equation. The phenomenological GEM equation [3], developed for randomly oriented ellipsoids, describes very nicely the electrical conductivity of composites containing asymmetric fibers. The

percolation phenomena were clearly observed since the difference of electrical conductivity between polymer and fiber is very large. The morphological variable  $t$  of the GEM equation decreased and thus the slopes of the electrical conductivity curves became steeper as the fiber aspect ratio increased. The steep

increase of conductivity is reasonable since easier percolation is expected for the longer fiber.  $V_c$  decreased from 5.79 to 2.36% as the fiber AR increased from 4.0 to 10.3. For the 3-dimensional conductor-insulator composites of closed-packed hard spheres of equal size, the  $V_c$  value is close to 16% for

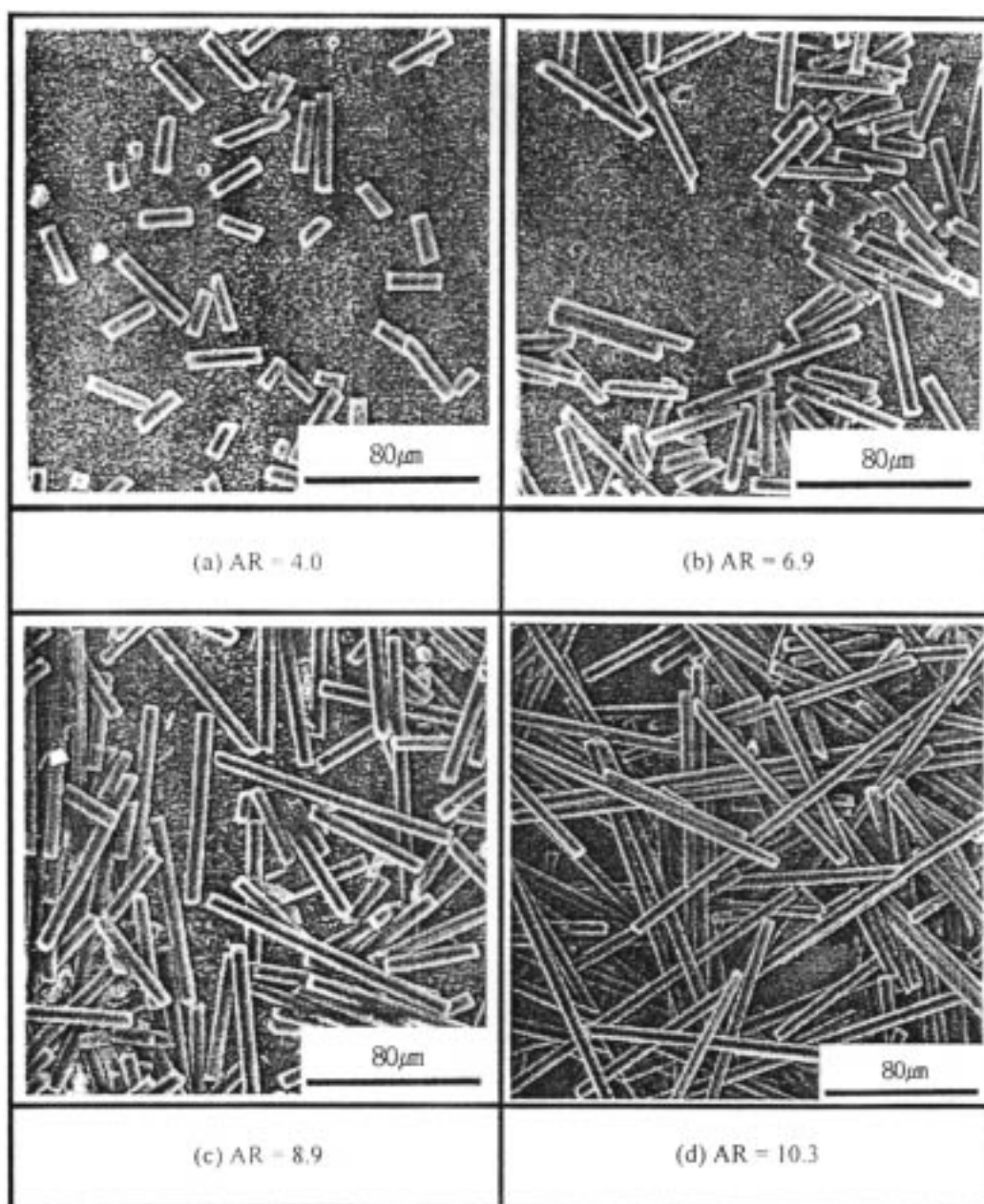


Fig. 1. Optical micrographs of crushed and sieved carbon fibers with the aspect ratio (AR) of (a) 4.0, (b) 6.9, (c) 8.9 and (d) 10.3.

most lattices [3]. The smaller  $V_c$  values for the present samples are due to the fibers instead of spherical particles and also to the non-random arrangement of second phase.

The effect of aspect ratio of fiber on the  $V_c$  values in this study and the results of simulations [21–24] and experiment [4] in other studies are compared in Fig. 5.

The simulations were based on either 2-D lattices [21,22] or 3-D lattices [23,24]. The curves are wide spread in the graph and the present data are located near the lower-left corner of the plot, indicating smaller  $V_c$  for the same aspect ratio. Horizontal bars indicate the standard deviation of the fiber aspect ratio. For the aspect ratio, e.g., 10, the  $V_c$  value of this

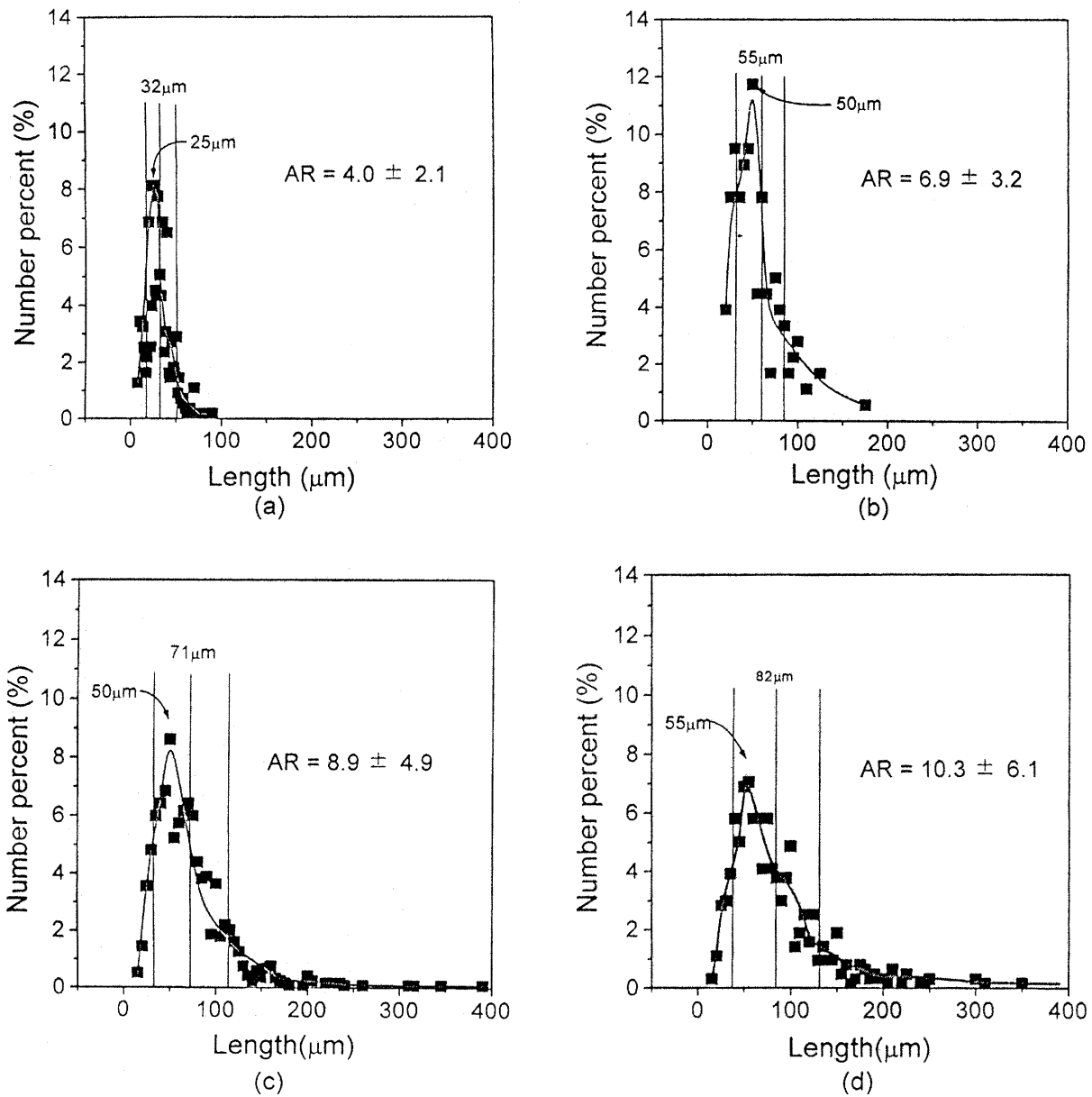


Fig. 2. Size distribution of carbon-fibers for aspect ratio of (a) 4.0, (b) 6.9, (c) 8.9, and (d) 10.3. The most frequent size and the average size were also indicated.

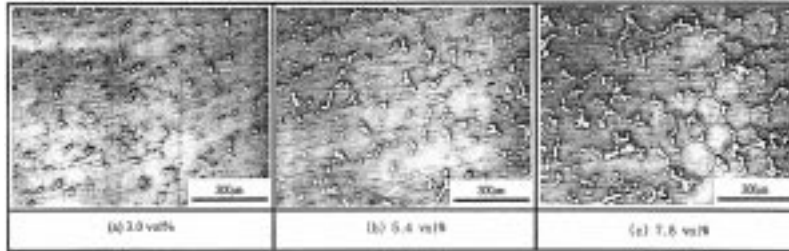


Fig. 3. Optical micrographs of polished surfaces of carbon fiber-polymer composites for various carbon-fiber contents of (a) 3.0, (b) 5.4, and (c) 7.8 vol. % with the fiber aspect ratio fixed at 6.9. Dotted circles in (c) were drawn to indicate the position of polymer particle.

study is 2.2, but those of other studies [4,21–24] vary from 16 to 24. The difference in  $V_C$  values may be due to the difference in the microstructure. Both the aluminum fibers in an experiment [4] and disks or sticks in computer simulations [21–24] were randomly distributed in the matrix without any constraints. Thus the fillers (fiber, disks or sticks) can be located in any position of the composite.

However, in this study, as shown in Fig. 3, fibers are located at the boundaries of polymer particles with little penetration into the polymer particles. Thus three-dimensional connection of fibers starts at lower fiber content compared to the situation with fibers distributed randomly throughout a sample without segregation at grain boundaries. Figure 6 shows a schematic figure of the microstructure of composites with their fibers segregated at grain boundaries and with their fibers randomly distributed throughout the sample. Fig. 6(a) shows the present microstructure obtained without melting the polymer. On the other hand, the microstructure shown in Fig. 6(b) has been

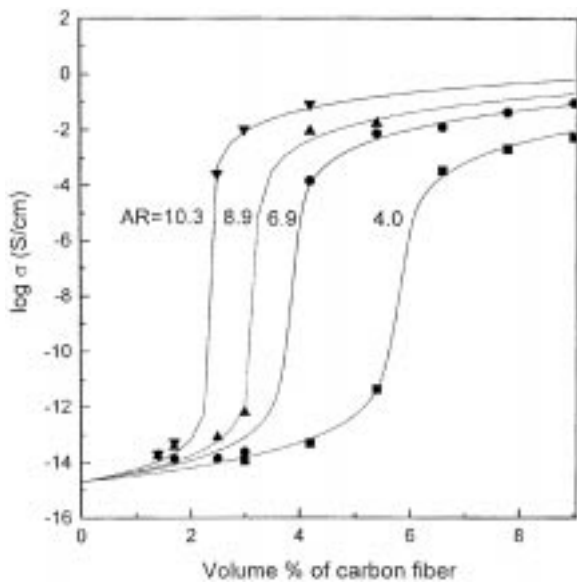


Fig. 4. The electrical conductivity of carbon fiber-polymer composites with various aspect ratios (AR) as a function of volume percent of carbon fiber. Curves were fitted with general effective medium equation.

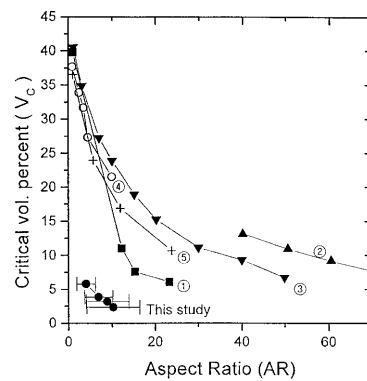


Fig. 5. Plot of the critical volume percent ( $V_c$ ) vs. aspect ratio (AR) for the present and other studies. Circled numbers indicate references; ① Bigg [4], ② Ueda & Taya [21], ③ Holm & Cima [22], ④ Bondt et. al. [23], ⑤ Ogale & Wang [24]. ① is an experimental result and ②–⑤ are from computer simulations.

Table 1. The morphological variable,  $t$  and  $V_c$ , for carbon fiber-polymer composites were determined by fitting general effective medium (GEM) equation [3] for the different aspect ratio of carbon fiber. The electrical conductivity values of polymer and carbon fiber are  $2 \times 10^{-5}$  and 93 S/cm, respectively

Aspect ratio	4.0	6.9	8.9	10.3
$V_c$ (%)	5.79	3.84	3.19	2.36
$t$	2.74	2.42	2.20	1.86

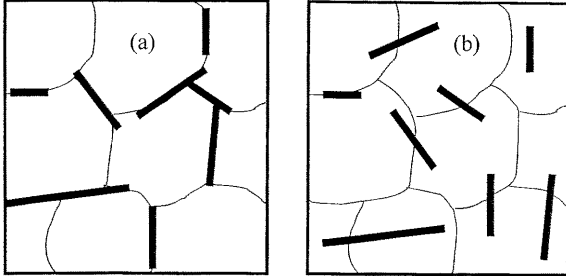


Fig. 6. Schematic diagrams showing microstructures for (a) fibers segregated at grain boundaries (this study), and (b) fibers distributed randomly throughout the sample (other studies).

obtained in other studies by mixing conductive fibers in molten polymers. It is thus clear that the microstructure shown in Fig. 6(a) will have much easier connection between fibers and lower percolation threshold concentration.

Figure 7 shows a plot of the inverse ( $V_c^{-1}$ ) of critical volume percent versus aspect ratio (AR) of fiber. The data shown in Fig. 5 were plotted again in this new graph by using a formula:

$$1/V_c = A + B (AR) \quad (4)$$

where  $A, B$  are fitting parameters. The straight lines are the best fitting curves. All data were fitted nicely with Eq. 4 and the fitting parameters  $A, B$  and the correlation coefficients of fitting are shown in Table 2. The excluded volume theory of percolation predicts that the critical volume fraction or percolation threshold concentration,  $V_c$ , of randomly distributed three-dimensional capped cylinders or fibers of length  $l$  and diameter  $d$  should follow [15]

$$V_c \propto \frac{\text{Vol}_f}{\text{Vol}_{\text{ex}}} \propto \frac{\frac{1}{6}\pi d^3 + \frac{1}{4}\pi d^2 \lambda}{\frac{4}{3}\pi d^3 + 2\pi d^2 \lambda + 2d\lambda^2 \langle \sin \gamma \rangle} \quad (5)$$

Table 2. Fitting parameters for the inverse relationship between critical volume percent and aspect ratio of fibers in various studies. Fitting equation is given by  $(V_c)^{-1} = A + B (AR)$  where  $V_c$  is a critical volume concentration of fibers and AR is an aspect ratio,  $A, B$  are fitting parameters.  $R$  is the correlation coefficient of the fitting.  $A, B$  values are based on volume fraction concentration, they should be multiplied by  $10^{-2}$  for volume percent concentration as shown in Fig. 7

Notation in Figs. 5 and 7	$A$	$B$	$R$
This study	1.13	3.75	0.969
① Bigg [4]	1.98	0.645	0.988
② Ueda & Taya [21]	1.06	0.167	0.997
③ Holm & Cima [22]	1.90	0.243	0.994
④ Bondt et al. [23]	2.50	0.218	0.983
⑤ Ogale & Wang [24]	2.47	0.291	0.999

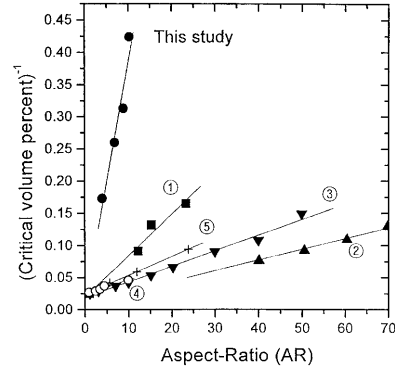


Fig. 7. Inverse relationship between critical volume concentration and aspect ratio. The circled numbers represent the same references shown in Fig. 5.

where  $\text{Vol}_f$  is the volume of a cylinder,  $\text{Vol}_{\text{ex}}$  is the average excluded volume of a cylinder,  $\gamma$  is the angle between axes of the two cylinders in three-dimensional space, the bracket  $\langle \rangle$  indicates the average value. For the cylinders of  $l \gg d$ , the  $l^2$  term dominates the denominator and  $V_c$  is proportional to  $d/l$ , which is the inverse of the aspect ratio. The spherical cap of cylinder has little effect on the dependence of  $V_c$  on the aspect ratio. Therefore, the excluded volume theory predicts that the  $V_c$  should be inversely proportional to the aspect ratio of the cylinders. It is shown in Fig. 5 and Fig. 7 that all the simulation data (②–⑤) [21–24] have higher  $V_c$  values as compared to the present experimental study or Bigg's experimental study (①) [4].  $V_c$  values in the present study are also smaller than for Bigg's results. It is known that the preparation conditions of the material, in addition to the aspect ratio, may affect strongly the value of  $V_c$  [25]. During fabrication, particles or fibers may form clusters in suspension of the molten polymer. The presence of clusters effectively reduces the  $V_c$  value. It has also been

predicted and experimentally shown that the surface tension of the polymer has an effect on particle coagulation [25]. The polymer with small surface tension favors particle clustering and thus decreases the  $V_c$  value. Thus experimental  $V_c$  values may always become smaller than the simulated values, which were obtained assuming completely random distribution of particles or fibers. In this context, the steep slope shown in Fig. 7 for the present study may be regarded as originating from the extreme clustering of fibers. The fibers were actually intentionally segregated to the interface region between polymer particles. Thus, as the degree of clustering or the segregation of fibers increases, the curve in Fig. 7 should move from near the horizontal position toward the vertical position.

Conductive fibers are either *particulates* or *fibers* and they can be either *randomly* distributed or *segregated* in a polymer matrix depending upon the status (molten or dry) of the polymer during preparation. Many theoretical and experimental studies focused on either random or segregated *particles* in the polymer matrix [26–28]. The  $V_c$  value of a composite with random particles can be dramatically reduced if the sizes of conductive particles are reduced with respect to the size of polymer particles. The composites with segregated particles also show the smaller  $V_c$  values than for the composites with random particles [26–28]. It was demonstrated [26] that the  $V_c$  could be reduced from 35% to 6% by segregating the spherical filler particles. The reduction of the  $V_c$  value is also possible if we substitute the random particles with random fibers. In order to obtain similar  $V_c$  values observed for the composite with segregated fibers, a very large size difference between filler and polymer particles is necessary. For example, to obtain a  $V_c$  value of about 2 vol.%, shown for the present composite of fiber aspect ratio 10, the  $R_p/R_m$  (polymer particle size/metal particle size) of the composite with segregated particles should exceed 30 [26–28]. Similarly, for aspect ratio 4, the required  $R_p/R_m$  values are 10 ~ 16. Since the fiber-filled composite requires less fillers for the same conductivity, the mechanical strength is expected to be higher for the composites with segregated fibers than for those with segregated particles. A decreasing mechanical strength is generally observed with the increasing volume fraction of added inorganic fillers [4,29]. Carbon

black, an example of small additive particles, is also difficult to process reliably and often degrades the mechanical properties of the composite. However, the mechanical strength of composites with segregated fibers may need to be compared with those with random fibers. This is because the strength of the fiber-polymer composite is dependent upon the distribution of fiber as well as the strength of fiber and the interfacial bond between the fiber and the matrix.

## Conclusions

Composites of carbon fibers and polymer particles were fabricated without melting the polymer. The aspect ratios of fibers were controlled by breaking long fibers. The critical volume concentration ( $V_c$ ) was determined as a function of fiber aspect ratio by measuring the electrical conductivity of the composites and fitting with GEM equation. The morphological variables,  $t$  of GEM fitting equations decreased and the slopes of the electrical conductivity curves increased as the fiber aspect ratio increased. The  $V_c$  value of the carbon-fiber-filled polymer composites decreased with increasing aspect ratio of carbon fiber.

The present composites with their fibers segregated between polymer particles showed much lower  $V_c$  values than those with their fibers located randomly throughout composites in other experimental or simulation studies. Although the present samples have segregated fibers with a limited range of aspect ratios, the relation between  $V_c$  and aspect ratio followed the inverse relation,  $V_c \propto (\text{AR})^{-1}$ , as expected in the prediction or computer simulations for the random fiber composite. Since the  $V_c$  value is expected to be a function not only of aspect ratio but also of the arrangement of fibers, further theoretical calculations to determine the  $V_c$  value of the composite should consider both factors.

## Acknowledgments

Supported by The Korea Science and Engineering Foundation, 1997 research fund. Carbon fibers were provided by Dr. Y.D. Park at the Research Institute of Industrial Science and Technology, Pohang, Korea.



## Note

Based in part on the thesis submitted by J.Y. Yi for the M.S. degree, Pohang University of Science and Technology, 1998.

## References

1. R.E. Newnham, *Chemtech*, Dec., 732 (1986).
2. R.E. Newnham, *Chemtech*, Jan., 38 (1987).
3. D.S. McLachlan, M. Blaszkiewicz, and R.E. Newnham, *J. Am. Ceram. Soc.*, **73**, 2187 (1990).
4. D.M. Bigg, *Poly. Eng. & Sci.*, **19**, 1188 (1979).
5. J.Y. Yi, M.S. Thesis, Pohang University of Science and Technology, Korea, 1998.
6. Y.M. Park and G.M. Choi, *J. Electrochem. Soc.*, **146**, 883 (1999).
7. Y.M. Park and G.M. Choi, *Sol. St. Ionics*, **120**, 265 (1999).
8. D.G. Han and G.M. Choi, *J. Electroceram.*, **2**, 57 (1998).
9. D.G. Han and G.M. Choi, *Sol. St. Ionics*, **106**, 71 (1998).
10. K. Wenderoth and J. Petermann, *Poly. Composites*, **10**, 52 (1989).
11. B.L. Lee, *Poly. Eng. and Sci.*, **32**, 36 (1992).
12. A. Larena and G. Pinto, *Poly. Composites*, **16**, 536 (1995).
13. S. Yoshikawa, T. Ota, and R. Newnham, *J. Am. Ceram. Soc.*, **73**, 263 (1990).
14. G.R. Ruschau, S. Yoshikawa, and R.E. Newman, *J. Appl. Phys.*, **72**, 953 (1992).
15. I. Balberg, C.H. Anderson, S. Alexander, and N. Wagner, *Phys. Rev. B*, **30**, 3933 (1984).
16. A.L.R. Bug, S.A. Safran, and I. Webman, *Phys. Rev. B*, **33**, 4716 (1986).
17. E. Charlaix, E. Guyon, and N. River, *Sol. St. Comm.*, **50**, 999 (1984).
18. E.D. Sichel, *Carbon black-polymer composites* (Marcel Dekker, Inc., New York, 1982), p. 7.
19. E.H. Immergut, *Polymer Handbook*, 3rd ed. (John Wiley & Sons Inc., New York, 1989), pp. V5-V7.
20. J. Donnet and R.C. Bansal, *Carbon Fibers* (Marcel Dekker, Inc., New York 1984), p. 201.
21. N. Ueda and M. Taya, *J. Appl. Phys.*, **60**, 459 (1986).
22. E.A. Holm and M.J. Cima, *J. Am. Ceram. Soc.*, **72**, 303 (1989).
23. S. De Bondt, L. Froyen, and A. Deruyttere, *J. Mater. Sci.*, **27**, 1383 (1992).
24. A.A. Ogale and S.F. Wang, *Comp. Sci. & Tech.*, **46**, 379 (1993).
25. F. Carmona, *Physica A*, 461 (1989).
26. A. Malliaris and D.T. Turner, *J. Appl. Phys.*, **42**, 614 (1971).
27. R.P. Kusy, *J. Appl. Phys.*, **48**, 5301 (1977).
28. S.F. Wang and A.A. Ogale, *Comp. Sci. & Tech.*, **46**, 93 (1993).